Intrinsic admittance of unipolar double-barrier resonant-tunneling structures

A. Kindlihagen
Department of Physics and Measurement Technology, University of Linköping, S-58183 Linköping, Sweden

A. G. Mal'shukov
Institute of Spectroscopy, Russian Academy of Science, 142092, Troitsk, Moscow Region, Russia

K. A. Chao
Department of Physics, Norwegian Institute of Technology, Norwegian University of Science and Technology, N-7034 Trondheim, Norway
and Department of Theoretical Physics, Lund University, S-22362 Lund, Sweden

M. Willander
Physical Electronics and Photonics, Department of Physics, Chalmers University of Technology, S-412 96 Göteborg, Sweden
(Received 21 March 1997; revised manuscript received 11 July 1997)

Following the definition of admittance, we have performed a theoretical analysis of the total intrinsic admittance of unipolar double-barrier resonant-tunneling structures. The theory includes contributions from the tunneling currents through the barriers, as well as from the charge distribution. We have solved the problem numerically for small ac voltage amplitudes in the framework of linear response. The calculations are fully quantum mechanical in the Hartree approximation. In linear response, and at frequencies much smaller than the internal frequencies of the system, the susceptance is found to be entirely of a capacitive nature. We have studied both a symmetric and a highly asymmetric sample, with a thick second barrier at the collector side. For the symmetric sample we found that the susceptance-voltage characteristic depends strongly on both frequency and temperature. A δ-shaped peak in the susceptance is found in the negative differential resistance region, where the conductance also depends strongly on frequency. For the asymmetric sample the susceptance exhibits a sharp maximum in the negative differential resistance region, although its value is smaller than that for the symmetric case. The frequency dependence of the susceptance is also found to be quite weak for the asymmetric sample. [S0163-1829(98)04939-X]

I. INTRODUCTION

In resonant tunneling the *current-voltage (I-V)* and the *capacitance-voltage (C-V)* characteristics are of basic importance. While the dc *I-V* characteristics of resonant tunneling structures are much studied, both the *C-V* characteristics and the inductive behavior are far from being fully understood. One important application of resonant tunneling structures is high-speed devices such as high-frequency oscillators and detectors. To understand the high-frequency behavior of these devices, it is essential to know the intrinsic admittance of the system.

The *C-V* characteristics of resonant tunneling structures are generally highly nonlinear and show the fingerprint of the quantum confinement, the so-called *quantum capacitance*. The notion of quantum capacitance was first introduced by Luryi.[1] Other authors have investigated the quantum capacitance in structures such as ordinary heterojunctions,[2] δ-doped structures,[3] quantum dots,[4] and interband tunneling structures,[5] as well as ordinary tunneling structures.[1,6–10] By ordinary tunneling structures we mean both the double-barrier resonant-tunneling structures[1,6–9] (DBRTS's) and the superlattice structures.[10]

There exists very little experimental work on the admittance of the unipolar DBRTS. However, there are two striking experiments, one on quantum dots,[4] and one on a superlattice structure,[10] which both demonstrate very high and narrow features of the admittance spectrum. In both cases the sharp peaks were interpreted as an intrinsic feature of resonant tunneling.

The existing theoretical treatments of the quantum capacitance vary from mostly classical approaches to methods based on quantum mechanics. Luryi[1] adapted the classical geometric capacitance of a three-plate parallel plate capacitor to the DBRTS. Genoe *et al.*[6] refined this model, by including the tunneling processes through the two barriers. Hu and Stapleton[7] proposed another definition of the quantum capacitance of DBRTS's, namely, $C=dQ_w/dV$, where Q_w is the charge in the quantum well and V the applied voltage. In a later work they included contributions from all *injected charge*.[9] These studies are all based on the quasistatic steady-state picture.

Investigations of the inductance of the DBRTS,[11,12] or more generally, the admittance,[13–15,17,16] have also been carried out. As a result of these studies there has been a controversy on whether the DBRTS is of dominantly capacitive or inductive nature. However, this controversy takes place only when one tries to apply conventional definitions of capacitance or inductance to tunneling systems with an ac voltage applied. For example, the conventional way to find the capacitance is based on defining the regions where charge is stored. These regions are considered as plates of a capacitor.

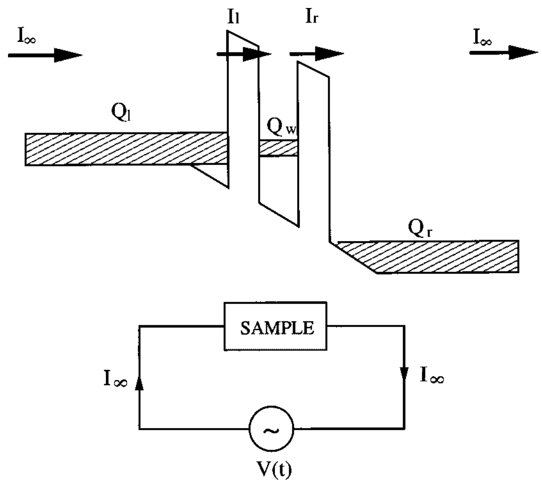

FIG. 1. Schematic sketch of the unipolar DBRTS (upper part) and a principal sketch of the ac circuit (lower part).

However, in tunneling systems there is no way to unambiguously define such regions. On the other hand, a consistent way to find the capacitance, as well as the inductance, can be based on an analysis of the complex admittance of the system. In a general ac circuit with an ac voltage $V(t) = V\sin\,\omega t$ and a complex admittance Y, the current is given by $I(t)=YV(t)$. The current may be separated into an *in-phase* part and an *out-of-phase* part $I(t)=I^{IP}(t)+I^{OP}(t)$. I^{IP} gives us the conductance $G=\mathrm{Re}(Y)$ and I^{OP}, which is 90° out of phase with the applied voltage, gives us the susceptance $B=\mathrm{Im}(Y)$. All information about capacitive and inductive characteristics of the system is contained in the frequency dependence of $B(\omega)$. In its turn, as seen from Fig. 1, the total current $I(t)$ corresponds to the measurable current I_∞. That allows for measurement of both the real and imaginary parts of the admittance.

Our goal is to develop a theory for calculating the complex admittance of a unipolar DBRTS in a wide enough region of ac frequencies. There have been several works approaching this problem. Some authors have employed Green's-function techniques based on the Landau-Büttiker formula,[11] the independent particle model with conventional tunneling theory,[12] and an analytic path-integral method.[14] None of these studies has taken into account the self-consistent potential in the sample. Other approaches, which are also not self-consistent, are the Liouville equation combined with the Wigner distribution,[13] the Breit-Wigner expansion of sidebands near resonances,[15] and the solution of the periodic time-dependent Schrödinger equation.[16] A self-consistent approach in the Hartree approximation, employing the harmonic balance technique was also reported.[17] However, in this work the transport of electrons was described by coherent tunneling, and thus the scattering processes of electrons in the quantum well were completely neglected.

While various levels of approximations have been employed to investigate the admittance of the DBRTS, none of them seems to be able to provide a sufficiently rigorous quantum-mechanical self-consistent approach allowing for an analysis of the capacitive and inductive nature of the admittance and comparing with experiment. In the present work we derive an exact equation for the admittance, expressing it via the tunneling currents and the charge distribution. For a small ac voltage superimposed onto a steady-state dc bias we derive a closed differential equation for the charge in the quantum well. In linear response the parameters of this equation will be calculated from a self-consistent steady-state solution of the system. After the charge inside the well is found we can determine the current across the system and so the complex admittance of the DBRTS. Our calculations allow us to provide a numerical treatment and qualitative explanation of the δ-shaped peaks in the admittance observed experimentally.[4] To our knowledge, this fundamental way of describing the total intrinsic admittance of tunneling structures is given for the first time. We would like to point out that the admittance peak appears in the bias voltage region for *negative differential resistance*. Therefore, in a way the admittance peak is associated to the resonant tunneling current through a unipolar DBRTS. As shown in some early calculation,[18] the transmission probability of an electron exhibits sharp peaks when the energy of the electron is close to the resonant levels in the well.

The paper is organized as follows. In Sec. II we define the system under consideration and develop the theoretical model for quantum admittance. The theory is then employed for numerical studies of two different samples in Sec. III. Finally we give some comments in Sec. IV. In the Appendix we demonstrate the correct symmetry property in our derivation of the quantum admittance.

II. LINEAR RESPONSE OF QUANTUM ADMITTANCE

We consider the unipolar DBRTS schematically illustrated in Fig. 1. The *sample* in the circuit is the DBRTS. The charge Q_l in the left reservoir, the current I_∞ in the left contact, and the tunneling current I_l through the left barrier satisfy the equation

$$\frac{dQ_l}{dt}=I_\infty(t)-I_l(t). \tag{1}$$

If we rewrite Eq. (1) as

$$I_\infty(t)=I_l(t)+\frac{dQ_l}{dV}\frac{dV}{dt}, \tag{2}$$

making use of the general definition of admittance it becomes

$$I_\infty(t)=I_l^{IP}(t)+I_l^{OP}(t)+\frac{dQ_l}{dV}\frac{dV}{dt}=\mathrm{Re}(Y)V\sin\,\omega t + \mathrm{Im}(Y)V\cos\,\omega t. \tag{3}$$

The *in-phase* component gives the conductance

$$\mathrm{Re}(Y)=G=\frac{I_l^{IP}}{V\sin\,\omega t}, \tag{4}$$

and the *out-of-phase* components give the susceptance

$$\mathrm{Im}(Y)=B=\omega\left(\frac{I_l^{OP}}{dV/dt}+\frac{dQ_l}{dV}\right). \tag{5}$$

We have derived the above results by analyzing the currents at the left part of the DBRTS shown in Fig. 1. Exactly the same results can be derived if we analyze the currents at the right part of the DBRTS, as one expects. This is shown in the Appendix.

To proceed further, we consider the situation of a small amplitude ac voltage, $\delta V(t)$, superimposed on a steady state dc bias V_0

$$V(t)=V_0+\delta V(t)=V_0+\delta V \sin \omega t. \tag{6}$$

For a typical density 2.5×10^{11} cm^{-2}, the hot electron relaxation time is less than 10^{-13} s.[19] On the other hand, the lifetime of an electron occupying the quasibound level in the well is of the order of the inverse tunneling rate, which is typically about 10^{-12} s. For the problem of our interest, the frequency ω is assumed to be sufficiently low such that the period of bias voltage variation is longer than the hot electron relaxation time. Therefore, the quasiequilibrium in the quantum well can be established since the lifetime of electron is sufficiently long as compared to the hot electron relaxation time. This quasiequilibrium state is characterized by a quasi-Fermi level. With given tunneling rates, quasi-Fermi level, and bias voltage, one can write the tunneling currents $I_l(t)$ and $I_r(t)$ as

$$I_l(t)=\frac{2e}{(2\pi)^3}\int d\mathbf{k} v_l(\mathbf{k})|t_l(\mathbf{k})|^2 \times[f(\mathbf{k};V,E_{f,l},T)-f(\mathbf{k};V,E_{f,w},T)]$$

$$I_r(t)=\frac{2e}{(2\pi)^3}\int d\mathbf{k} v_r(\mathbf{k})|t_r(\mathbf{k})|^2 f(\mathbf{k};V,E_{f,w},T).$$

We notice that the quasi-Fermi level is uniquely determined by the density of electrons in the quantum well. Therefore, $I_l(t)$-$I_r(t)$ is a function of $V(t)$ and $Q_w(t)$ at the same time because here ω is much less than the hot electron relaxation rate. This allows us to construct a closed differential equation for the charge Q_w in the quantum well,

$$\frac{dQ_w}{dt}=I_l(V,Q_w)-I_r(V,Q_w). \tag{7}$$

We assume $\delta V/V_0 \ll 1$, and in regions where $I_{l/r}(V)$ is fairly linear, we can safely treat the system in the framework of linear response. In this case the charge in the quantum well can be written as

$$Q_w(t)=Q_{w,0}+\delta Q_w(t), \tag{8}$$

where $Q_{w,0}$ is the dc response charge. Under steady state the two tunneling currents are equal,

$$I_l(V_0,Q_{w,0})-I_r(V_0,Q_{w,0})=0. \tag{9}$$

Using this condition the differential equation (7) is linearized as

$$\frac{d\,\delta Q_w}{dt}=\left.\frac{\partial(I_l-I_r)}{\partial V}\right|_{(V_0,Q_{w,0})}\delta V(t)+\left.\frac{\partial(I_l-I_r)}{\partial Q_w}\right|_{(V_0,Q_{w,0})}\delta Q_w(t)$$
$$\equiv\Gamma\,\delta V \sin \omega t+\Omega\,\delta Q_w(t), \tag{10}$$

where the coefficients Γ and Ω are the corresponding partial derivatives evaluated at steady state. We are interested in the solution of $\delta Q_w(t)$ in response to an ac voltage of frequency ω. Consequently the solution of Eq. (10) has the form

$$\delta Q_w(t)=-\frac{\Gamma\,\delta V}{\omega^2+\Omega^2}(\omega \cos \omega t+\Omega \sin \omega t). \tag{11}$$

Our scheme for calculating the conductance and the susceptance, defined in Eqs. (4) and (5), is to calculate self-consistently the charge distribution and the tunneling currents at steady-state for all voltages V_0. From this steady-state solution, within the linear response regime, we are ready to derive dQ_l/dV, as well as the coefficients Γ and Ω defined in Eq. (10). With these coefficients, $\delta Q_w(t)$ in Eq. (11) is obtained. We can then calculate the time-dependent current $I_l(t)$ and separate the two components $I_l^{IP}(t)$ and $I_l^{OP}(t)$. Now we have obtained all quantities required for calculating the conductance (4) and the susceptance (5).

Let us first clarify the question that the nature of the susceptance (5) is capacitive or inductive. The last part of Eq. (5), $\omega dQ_l/dV$, is clearly a regular linear function of frequency, and thus contributes capacitively to the susceptance. The more interesting part of (5) is $(\omega I_l^{OP})/(dV/dt)$. From our detailed numerical calculations this part is found to be proportional to $\omega/(\omega^2+\Omega^2)$. There are two different regimes to be considered, $\omega\ll\Omega$ and $\omega\gg\Omega$. Ω was defined in Eq. (10) as $\partial(I_l-I_r)/\partial Q_w$, and plays the role of the typical *internal frequency* of the system. Let us first look at the low-frequency limit $\omega\ll\Omega$. By expanding $\omega/(\omega^2+\Omega^2)$ in powers of ω at small frequencies one finds a regular series of odd positive powers with a leading linear term. Inductance is, however, identified with a singular term diverging as $1/\omega$. Consequently, for $\omega\ll\Omega$, the susceptance (5), when calculated in linear response, is of a purely capacitive nature. This is exactly the conclusion expected from a linear response theory. In the high-frequency limit, $\omega\gg\Omega$, the situation is more complicated. The regular part from dQ_l/dV still contributes to the capacitance. However, the term $(\omega I_l^{OP})/(dV/dt)$ will go as $1/\omega$, and thus be of inductive nature. For $\omega\to\infty$ this term vanishes, and we are left with only the capacitive term $C_\infty\equiv dQ_l/dV$.

To conclude our theoretical analysis we give a brief description of our self-consistent calculation for the steady state. The method is described in detail elsewhere for a more complicated bipolar DBRTS.[20] We consider the heavily doped emitter and collector as perfect particle reservoirs, characterized by their respective Fermi energies. Assuming a quasi-Fermi level in the well, we solve the Poisson and Schrödinger equations self-consistently, together with the equations for the two tunneling currents I_l and I_r. The constraint (9) on the two tunneling currents determines the steady-state quasi-Fermi energy in the quantum well, and thus the steady-state charge $Q_{w,0}$. With this self-consistent steady state we proceed to calculate the admittance as described earlier.

III. NUMERICAL RESULTS

We have studied both a symmetrical and a highly asymmetrical DBRTS. We will first present the numerical results for the symmetrical DBRTS (sample A), the structure of

TABLE I. Structure of sample A (for Figs. 2–7).

Emitter	2×10^{18} n^+ GaAs	400 Å
Spacer	undoped GaAs	80 Å
Barrier	undoped $Al_{0.3}Ga_{0.7}As$	40 Å
Well	undoped GaAs	50 Å
Barrier	undoped $Al_{0.3}Ga_{0.7}As$	40 Å
Spacer	undoped GaAs	80 Å
Collector	2×10^{18} n^+ GaAs	400 Å

which is described in Table I. In Fig. 2 we show both $\mathrm{Im}(Y)/\omega$ and the steady-state current as functions of voltage at $T=300$ K. $\mathrm{Im}(Y)/\omega$ is plotted for both the low frequency $\omega=10^3$ s^{-1} and the high frequency $\omega=10^{12}$ s^{-1}. It is important to point out that in the limit $\omega\rightarrow0$, $\mathrm{Im}(Y)/\omega$ has contributions from the current terms in Eq. (5), and therefore is different from the steady-state result dQ_l/dV. For both the high and the low frequency, the susceptance exhibits a sharp, almost δ-shaped, peak at bias voltage $V_0=0.3$ V, which lies right in the middle of the *negative differential resistance* (NDR) region. The δ spike originates from the discharging of the quantum well, and is a fingerprint of the *quantum admittance*. Such sharp peak in the susceptance has been found in DBRTS's,[6,7,15,17,16] in superlattices,[10] and in quantum dots.[4] Besides the main sharp peak, we observe a pronounced drop of $\mathrm{Im}(Y)/\omega$ when the voltage increases across 0.18 V. The reason for this drop is that at this bias voltage the tunneling becomes resonant, i.e., the energy level in the quantum well coincides with the Fermi energy in the emitter. For low frequency we also see a small drop in $\mathrm{Im}(Y)/\omega$ at the voltage $V_0=0.12$ V. The mechanism of this drop is hidden in the term $\partial I_r/\partial Q_w$ in Eq. (10), and cannot be explained by a simple physical picture.

The conductance is calculated as $G(V,\omega)=G_0+\delta G$, where the steady-state conductance is given by $G_0=I_l(V_0,Q_{w,0})/V_0$ and $\delta G=\delta I_l^{IP}(t)/\delta V\sin\omega t$, with $\delta I_l^{IP}(t)$ derived from $\delta Q_w(t)$ in Eq. (11). The conductance-voltage relation at $T=300$ K is shown in Fig. 3, with the solid curve for the high frequency $\omega=10^{12}$ s^{-1}, the dashed curve for the low frequency $\omega=10^3$ s^{-1}, and the dash-dotted curve for the steady-state conductance. The conductance has large

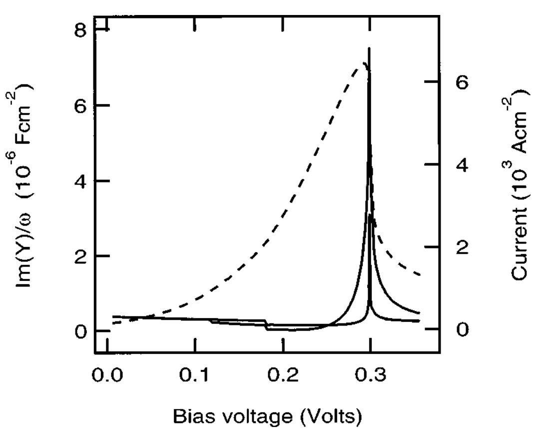

FIG. 2. $\mathrm{Im}(Y)/\omega$ for the low frequency $\omega=10^3$ s^{-1} (curve with the higher δ peak), the high frequency $\omega=10^{12}$ s^{-1} (curve with the lower δ peak), and the steady-state current (dashed curve) as functions of voltage at temperature $T=300$ K for sample A.

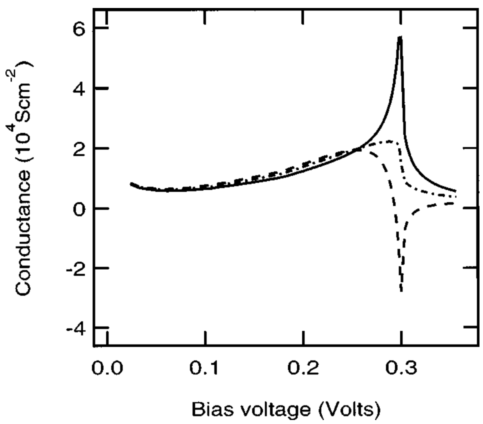

FIG. 3. Conductance-voltage characteristics for the low frequency $\omega=10^3$ s^{-1} (dashed curve), the high frequency $\omega=10^{12}$ s^{-1} (solid curve), and the steady-state (dash-dotted curve) for sample A at temperature $T=300$ K.

contributions from δG in the NDR region around 0.3 V, which makes $G(V,\omega\rightarrow0)$ different from the steady-state conductance. As a result of this, the overall conductance in the NDR region is negative for low frequencies and positive for high frequencies. This agrees well qualitatively with results obtained by others.[13,15,17,16]

We have reproduced Fig. 2 for various temperatures in order to investigate the temperature dependence of the susceptance. Again we are most interested in the NDR region, within which $\mathrm{Im}(Y)/\omega$ exhibits a δ peak at an optimal bias voltage. Both the value of the optimal voltage and the magnitude of the δ peak are found to be strongly temperature dependent as shown in Figs. 4 and 5. In Fig. 4 we see that as the temperature increases the optimal voltage remains constant for very low temperatures $T<50$ K, and then decreases linearly with temperature. Such behavior is due to the temperature dependence of the self-consistently derived resonant energy level in the quantum well. With increasing temperature, the charge accumulation in the well increases and so the resonant energy level drops. Therefore it requires a lower bias voltage to reach the NDR regime, in which lies the δ peak of the susceptance. The optimal bias voltage is frequency independent, as seen from the low- and the high-frequency curves for $\mathrm{Im}(Y)/\omega$ in Fig. 2.

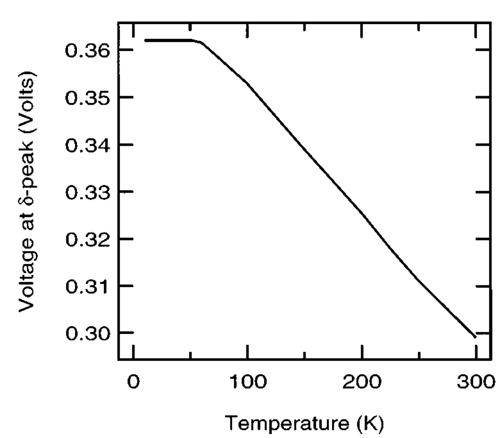

FIG. 4. Temperature dependence of the optimal bias voltage for the occurrence of the δ peak in $\mathrm{Im}(Y)/\omega$ for sample A.

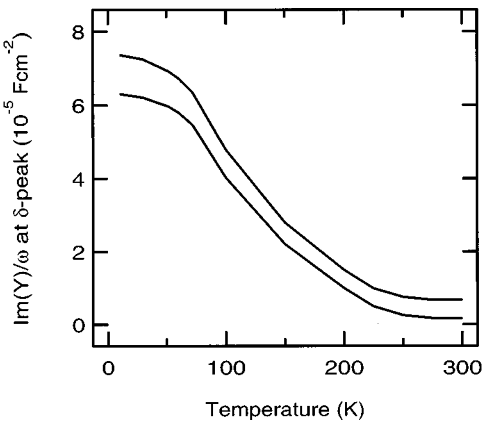

FIG. 5. Temperature dependence of the magnitude of the δ peak in $\mathrm{Im}(Y)/\omega$ for the low frequency $\omega = 10^3\ \mathrm{s}^{-1}$ (upper curve) and the high frequency $\omega = 10^{12}\ \mathrm{s}^{-1}$ (lower curve) for sample A.

In Fig. 5 we plot the magnitude of the δ peak of $\mathrm{Im}(Y)/\omega$ as a function of temperature for the low frequency $\omega = 10^3\ \mathrm{s}^{-1}$ (upper curve) and the high frequency $\omega = 10^{12}\ \mathrm{s}^{-1}$ (lower curve). In both cases the peak height decreases with temperature. This is exactly what one would expect, since with increasing temperature the NDR region in the *I-V* curve gets broader. The broadening of the NDR region reduces the discharging of the quantum well, and consequently decreases the δ peak in $\mathrm{Im}(Y)/\omega$.

In the NDR region, for a fixed temperature, the admittance is very sensitive to the frequency as seen in Figs. 2 and 3. We have investigated this frequency dependence in detail, and the results are given in Figs. 6 and 7 for sample A at the bias voltage 0.3 V and the temperature $T = 300$ K. This is exactly the $T = 300$ K point in Fig. 4, and consequently the peak value of $\mathrm{Im}(Y)/\omega$ is plotted in Fig. 6, and the peak value of the conductance G is plotted in Fig. 7. The peak value of the admittance has a large contribution from the current term in Eq. (5), which is related to the charge in the quantum well given by Eq. (11). As expected from our theoretical analysis in the previous section, in Fig. 6 $\mathrm{Im}(Y)/\omega$ drops to a constant value $C_\infty = dQ_l/dV$ for $\omega \gg \Omega$, and become purely capacitive. For this sample A the internal frequency, at $T = 300$ K and voltage $V_0 = 0.3$ V, is $\Omega = 0.2 \times 10^{12}\ \mathrm{s}^{-1}$. This is in good agreement with the electron tunneling time of a few picoseconds, found in similar structures.[20,21] From Fig. 6 we see that $\mathrm{Im}(Y)/\omega$ has practically reached C_∞ at $\omega \approx 10^{12}\ \mathrm{s}^{-1}$, which is much larger than Ω.

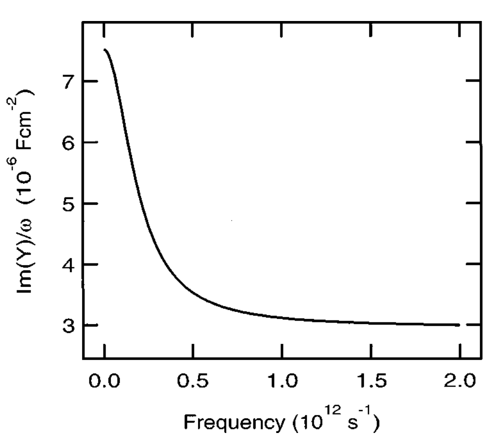

FIG. 6. Frequency dependence of $\mathrm{Im}(Y)/\omega$ at voltage 0.3 V and $T = 300$ K for sample A. Under these conditions $\mathrm{Im}(Y)/\omega$ has the peak value.

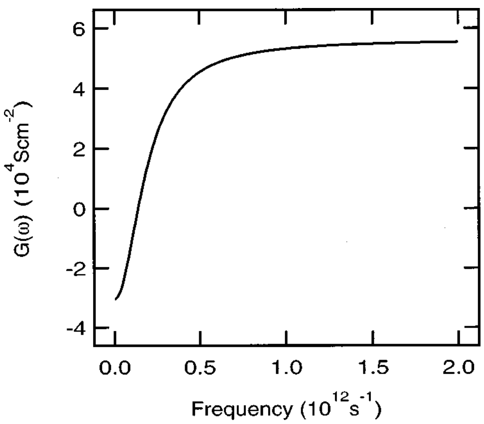

FIG. 7. Frequency dependence of the conductance at voltage 0.3 V and $T = 300$ K for sample A. Under these conditions $\mathrm{Im}(Y)/\omega$ has the peak value.

As mentioned at the beginning of this section, we use the formulation $G(V,\omega) = G_0 + \delta G$, where G_0 is the steady-state conductance, to calculate the conductance. With a tedious analysis we can show that δG has a frequency dependence of the form $(\omega^2 - \Omega^2)/(\omega^2 + \Omega^2)$. Therefore $G(V,\omega \to \infty) - G(V,\omega = \Omega) = G(V,\omega = \Omega) - G(V,\omega \to 0)$. For sample A at temperature $T = 300$ K and bias voltage 0.3 V, we found $\Omega = 0.2 \times 10^{12}\ \mathrm{s}^{-1}$ and $G(V,\omega = \Omega) = G_0 = 1.5 \times 10^4\ \mathrm{S\,cm}^{-2}$. All these features are confirmed in Fig. 7, where the conductance increases from a negative value to a positive saturation as the frequency increases from $\omega = 0$ to $\omega > \Omega$.

We have reached our conclusion that the characteristic features of the quantum admittance is related to the dynamics of the tunneling current, especially in the NDR region. We therefore expect a suppression of the quantum behavior of the admittance if the peak-to-valley ratio of the tunneling current is reduced. This can be achieved easily by increasing the strength of the barrier on the collector side, but at the same time to make sure there is no bistability. To demonstrate this point, let us consider the asymmetric DBRTS (sample B), the structure of which is specified in Table II. In Fig. 8 we plot $\mathrm{Im}(Y)/\omega$ of sample B for the low frequency $\omega = 10^3\ \mathrm{s}^{-1}$ at the temperature $T = 300$ K, together with the steady state *I-V* curve. Although in this case we also observe a relatively sharp peak in $\mathrm{Im}(Y)/\omega$ in the NDR region, it is

TABLE II. Structure of sample B (for Figs. 8 and 9).

Emitter	$2 \times 10^{18}\ n^+$ GaAs	400 Å
Spacer	undoped GaAs	80 Å
Barrier	undoped $Al_{0.3}Ga_{0.7}As$	50 Å
Well	undoped GaAs	60 Å
Barrier	undoped $Al_{0.3}Ga_{0.7}As$	100 Å
Spacer	undoped GaAs	80 Å
Collector	$2 \times 10^{18}\ n^+$ GaAs	400 Å

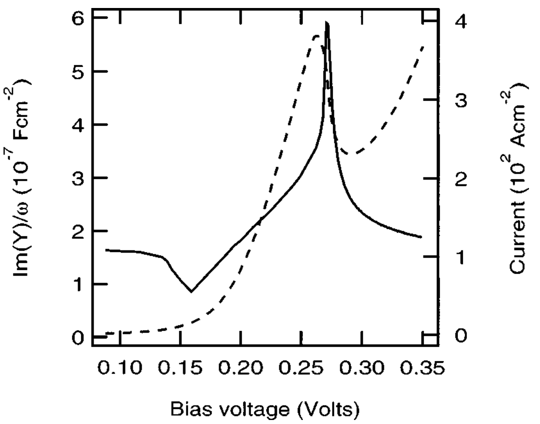

FIG. 8. $\mathrm{Im}(Y)/\omega$ for the low frequency $\omega=10^3\ \mathrm{s}^{-1}$ (solid curve) and the steady-state current (dashed curve) as functions of voltage at temperature $T=300$ K for sample B.

much broader and less intense as compared to the corresponding peak structure of the symmetric sample A, as shown in Fig. 2. These changes are due to a large reduction of the tunneling current and a dramatic broadening of the NDR region, as can be seen from the steady-state *I-V* curve in Fig. 8. The susceptance minimum appearing at $V_0=0.16$ V in Fig. 8 is caused by the onset of resonant tunneling, the same reason as for the susceptance drop at 0.18 V in Fig. 2.

The peak in $\mathrm{Im}(Y)/\omega$ in Fig. 8 is located at the bias voltage 0.27 V. The corresponding internal frequency is $\Omega=4.0\times10^{12}\ \mathrm{s}^{-1}$. We keep the bias voltage at 0.27 V and the temperature at $T=300$ K, but vary the frequency to calculate $\mathrm{Im}(Y)/\omega$ as function of frequency. The result is plotted in Fig. 9. By comparing Fig. 9 and Fig. 6, it is obvious that the change of the dynamics of the tunneling current affects this susceptance-frequency relation quantitatively but not qualitatively, as expected from Eq. (5).

IV. DISCUSSION

With Eqs. (4) and (5) we have provided the exact expression of the total intrinsic admittance of the unipolar DBRTS, derived from our theoretical analysis. The self-consistent numerical solutions are obtained within the framework of linear response. The use of linear response is well justified as long as (1) the ac amplitude δV is much less than the dc bias V_0, and (2) around this V_0 the tunneling current $I_{l/r}$ is fairly linear on the scale of δV. Under this approximation the susceptance was found to be of entirely capacitive nature for both $\omega\to0$ and $\omega\gg\Omega$. However, it would be of interest to go beyond the linear response approximation to investigate the inductive component of the susceptance as well as the nonlinear response of the DBRTS to a larger ac amplitude.

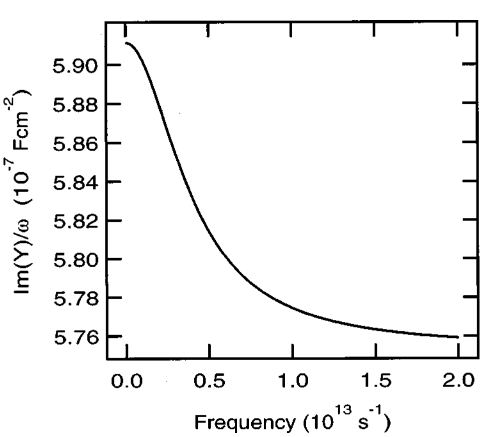

FIG. 9. Frequency dependence of $\mathrm{Im}(Y)/\omega$ at voltage 0.27 V and $T=300$ K for sample B. Under these conditions $\mathrm{Im}(Y)/\omega$ has the peak value.

Nevertheless, even with the nonlinear response neglected, when compared with the existing theoretical treatments on this subject, our fundamental way of describing the total intrinsic admittance of tunneling structures is given for the first time. Because our theory goes beyond all existing ones, our calculations produces for the first time the correct explanation of the δ-shaped peaks in the capacitance observed experimentally.[4] It is important to notice in Fig. 2 and Fig. 8 that the admittance peak appears in the bias voltage region for NDR. Therefore, the admittance peak is associated with the resonant tunneling current through a unipolar DBRTS. The resonant current peaks in Fig. 2 and Fig. 8 are broad because of the finite Fermi energy in the left reservoir in Fig. 1. If we let the Fermi energy approach zero to simulate the tunneling of a single electron with specific energy, as shown in some early calculations,[18] the transmission probability exhibits sharp peaks when the energy of the electron is close to the resonant levels in the well.

Since the phonon energy in GaAs, ~37 meV, is of the same order of magnitude as the thermal energy k_BT at room temperature, the phonon scattering, with a time constant $\sim10^{-13}$ s, will be a very effective process for fast relaxation of electrons in the quantum well and thus allow us to define the quasiequilibrium. Furthermore, our detailed numerical calculations has shown that in the entire bias voltage range under consideration, the electron density in the well is $\sim10^{11}\ \mathrm{cm}^{-2}$. For instance, for sample A at bias voltage 0.12 V the density is already $0.5\times10^{11}\ \mathrm{cm}^{-2}$, at voltage 0.3 V it has increased to $2\times10^{11}\ \mathrm{cm}^{-2}$ before it decreases again to $0.5\times10^{11}\ \mathrm{cm}^{-2}$ at 0.35 V. With such high densities of electrons in the well electron-electron scattering will be very strong. This will contribute to the fast relaxation of electrons, and thus further support our assumption of a quasiequilibrium in the quantum well.

The major deficiency in our solution of the steady-state problem is the lack of an explicit treatment of phonon scattering. The phonons smear out the sharp features of the *I-V* characteristics and give a broadening of the NDR region. Consequently we would expect a wider δ peak with a smaller amplitude in $\mathrm{Im}(Y)/\omega$. Furthermore, one can go beyond the Hartree approximation to include many-body effects. However we do not expect these improvements to alter the qualitative features of the quantum admittance demonstrated in this paper.

APPENDIX: SYMMETRY PROPERTIES OF QUANTUM ADMITTANCE

We will briefly repeat the analysis with Q_r instead of Q_l to derive the same results of conductance and susceptance as given by Eqs. (4) and (5). Analogous to (1) the charge Q_r and the currents I_r and I_∞ satisfy

$$\frac{dQ_r}{dt}=I_r(t)-I_\infty(t), \tag{A1}$$

which we rewrite as

$$I_\infty(t)=I_r^{IP}(t)+I_r^{OP}(t)-\frac{dQ_r}{dV}\frac{dV}{dt}. \tag{A2}$$

This give the conductance

$$\mathrm{Re}(Y)=G=\frac{I_r^{IP}}{V\sin\,\omega t}, \tag{A3}$$

and the susceptance

$$\mathrm{Im}(Y)=B=\omega\left(\frac{I_r^{OP}}{dV/dt}-\frac{dQ_r}{dV}\right). \tag{A4}$$

The two equivalent expressions for the susceptance, Eqs. (5) and (A4), are consistent with the charge conservation law

$$\frac{d}{dV}(Q_w+Q_l+Q_r)=0. \tag{A5}$$

To prove this we rewrite Eqs. (3) and (A2) as

$$I_\infty(t)-I_l^{IP}(t)=\frac{\mathrm{Im}(Y)}{\omega}\frac{dV}{dt},$$

$$I_\infty(t)-I_r^{IP}(t)=\frac{\mathrm{Im}(Y)}{\omega}\frac{dV}{dt}.$$

Since I_∞ for the left is identical to I_∞ for the right side of the sample, it is clear that $I_l^{IP}=I_r^{IP}$, which is simply the statement that the conductance of the DBRTS, Eqs. (4) and (A3), is uniquely defined regardless its derivation. We now consider the charge Q_w in the quantum well, which is related to the tunneling currents as

$$\frac{dQ_w}{dt}=I_l(t)-I_r(t)=I_l^{OP}(t)-I_r^{OP}(t).$$

By rewriting the above equation and making use of Eqs. (5) and (A4) we obtain the desired conservation law (A5),

$$\frac{dQ_w}{dV}=\frac{I_l^{OP}(t)-I_r^{OP}(t)}{dV/dt}=-\frac{d}{dV}(Q_l+Q_r).$$

[1] S. Luryi, Appl. Phys. Lett. **52**, 501 (1988).
[2] T. Jungwirth and L. Smrčka, Phys. Rev. B **51**, 10 181 (1995).
[3] M. E. Lazzouni and L. J. Sham, Phys. Rev. B **48**, 8948 (1993).
[4] R. C. Ashoori, H. L. Stormer, J. S. Weiner, L. N. Pfeiffer, S. J. Pearton, K. W. Baldwin, and K. W. West, Phys. Rev. Lett. **68**, 3088 (1992).
[5] K. Fobelets, R. Vounckx, J. Genoe, G. Borghs, H. Grönqvist, and L. Lundgren, Appl. Phys. Lett. **64**, 2523 (1994).
[6] J. Genoe, C. Van Hoof, W. Van Roy, J. H. Smet, K. Fobelets, R. P. Mertens, and G. Borghs, IEEE Trans. Electron Devices **38**, 2006 (1991).
[7] Y. Hu and S. Stapleton, Appl. Phys. Lett. **58**, 167 (1991).
[8] S. Luryi, Appl. Phys. Lett. **59**, 2335 (1991).
[9] T. Wei and S. Stapleton, J. Appl. Phys. **76**, 1287 (1994).
[10] Y. Zhang, Y. Li, D. Jiang, X. Yang, and P. Zhang, Appl. Phys. Lett. **64**, 3416 (1994).
[11] Y. Fu and S. C. Dudley, Phys. Rev. Lett. **70**, 65 (1993).
[12] N. Zou, M. Willander, and K. A. Chao, Phys. Rev. B **50**, 4980 (1994).
[13] W. R. Frensley, Appl. Phys. Lett. **51**, 448 (1987).
[14] L. Y. Chen and C. S. Ting, Phys. Rev. Lett. **64**, 3159 (1990).
[15] H. C. Liu, Phys. Rev. B **43**, 12 538 (1991).
[16] C. L. Fernando and W. R. Frensley, Phys. Rev. B **52**, 5092 (1995).
[17] W-R. Liou and P. Roblin, IEEE Trans. Electron Devices **41**, 1098 (1994).
[18] Carlo Jacoboni and Peter J. Price, Solid State Commun. **75**, 193 (1990).
[19] C. H. Yang, J. M. Carlson-Swindle, S. A. Lyon, and J. M. Worlock, Phys. Rev. Lett. **55**, 2359 (1985).
[20] A. Kindlihagen, K. A. Chao, and M. Willander, Semicond. Sci. Technol. **12**, 535 (1997).
[21] T. C. L. G. Sollner, W. D. Goodhue, P. E. Tannenwald, C. D. Parker, and D. D. Peck, Appl. Phys. Lett. **43**, 588 (1983).